Direct and indirect methods in optimal control with state constraints and the climbing trajectory of an aircraft

Olivier Cots, Joseph Gergaud, Damien Goubinat

OPTIMAL CONTROL APPLICATIONS AND METHODS
Optim. Control Appl. Meth. 0000; **00**:1–23
Published online in Wiley InterScience (www.interscience.wiley.com). DOI: 10.1002/oca

Direct and indirect methods in optimal control with state constraints and the climbing trajectory of an aircraft

O. Cots[1], J. Gergaud[1] and D. Goubinat[2*]

[1]*Toulouse Univ., INP-ENSEEIHT, IRIT & CNRS, 2 rue Camichel, F-31071 Toulouse, France*
[2]*Thales Avionics SA, 105 av du General Eisenhower, B.P. 1147, 31047 Toulouse Cedex, France*

SUMMARY

In this article, the minimum time and fuel consumption of an aircraft in its climbing phase is studied. The controls are the thrust and the lift coefficient and state constraints are taken into account: air slope and speed limitations. The application of the Maximum Principle leads to parameterize the optimal control and the multipliers associated to the state constraints with the state and the costate and leads to describe a Multi-Point Boundary Value Problem which is solved by multiple shooting. This indirect method is the numerical implementation of the Maximum Principle with state-constraints and it is initialized by the direct method, both to determine the optimal structure and to obtain a satisfying initial guess. The solutions of the boundary value problems we define give extremals which satisfy necessary conditions of optimality with at most two boundary arcs. Note that the aircraft dynamics has a singular perturbation but no reduction is performed.

Received ...

KEY WORDS: Geometric optimal control; state constraints; direct and indirect methods; aircraft trajectory.

1. INTRODUCTION

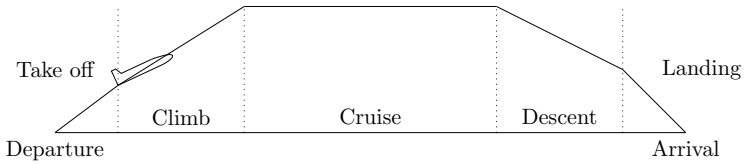

Figure 1. A flight divided into phases

A flight is composed of several phases which are take-off, climb, cruise, descent, approach and landing, see Figure 1. In this article, we are interested in the optimal control of an aircraft during its climbing phase. This phase is determined by its own dynamics given by an ordinary differential equation, constraints to comply with and a criterion to minimize. In this article, we consider a realistic model where the aircraft is described by its altitude h, its longitudinal distance d, the true air speed V, its mass m and the air slope γ, and where the data, as the air density, the temperature, the pressure, the maximal thrust of the aircraft and the fuel flow, are given by two standard models,

*Correspondence to: Thales Avionics SA, 105 av du General Eisenhower, B.P. 1147, 31047 Toulouse Cedex, France.
E-mail: damien.goubinat@enseeiht.fr

see section 2.1. Companies are trying to optimize the cost of the flight which is a combination of fuel consumption, time of flight and some environmental issues as noise. In this study, we define the objective function by a weighted sum of the two criteria: time of flight and fuel consumption.

This climbing phase has already been studied in [2, 28] but without taking into account any operational state constraints and with different criteria. In this article, we consider limitations on the air slope (the aircraft cannot go down) and on the Mach speed, which is commonly applied to protect the structure of the aircraft. In the reference [2], the author consider a simpler model without any state constraint and gives a very detailed analysis of the singular perturbation phenomenon which arise from the air slope dynamics. It is well known that the aircraft dynamics has slow (the mass m) and fast (the air slope γ) variables. The altitude h and the true air speed v are fast compare to the mass but slow compare to the air slope. This time scale separation is normally treated by a singular perturbation analysis where the solution is approximated by an asymptotic expansion. Ordinary differential equations with a singular perturbation have the particularity that the asymptotic expansion is non uniform with respect to the time. Hence, with this method, one has to consider at least two different time scales which leads to compute two different asymptotic expansions and then, in order to get a good approximation of the whole trajectory, the two asymptotic expansions has to be matched. We refer to [2, 21, 26, 29] for details about singular perturbation analysis. In [10], the same climbing phase is studied but with a simpler model and without any state constraints. The authors compare extremals of the original problem with extremals of its zero-order approximation. In this article, we intend to proceed to the first step, *i.e.* computing extremals satisfying necessary conditions of optimality for the original problem, taking into account state constraints. Thus, we focus our analysis on the non-reduced optimal control problem, which is a challenging problem because of the singular perturbation, the realistic dynamics model and the state constraints. On the other hand, we make some assumptions to reduce the complexity of the dynamics. For instance, compare to [28], we assume that we are in presence of a steady and horizontal wind field. We refer to [15] for a detailed description of the aircraft dynamics.

The underlying optimal control problem is in Mayer form with a state variable of dimension five, with two controls (the lift coefficient C_L and the normalized amount of thrust ε) and two state constraints. The associated Hamiltonian is affine with respect to ε and quadratic with respect to C_L. The solution of this optimal control problem can be found as an extremal solution of the maximum principle with state constraints, [19, 23, 25, 31]. The associated optimal strategy is a concatenation of boundary and interior arcs. Each type of arc is fully characterized by the application of the maximum principle and we use first a direct method to determine the structure of the optimal trajectory. Roughly speaking, the direct methods based on state and control parameterization consist in making a full discretization of the optimal control problem and then using numerical algorithms to compute candidate points which satisfy the Kuhn-Tucker conditions, see [3, 14, 33] for details. On the other hand, for a given structure, the application of the maximum principle leads to the formulation of a Multi-Point Boundary Value Problem (MPBVP). Solving the MPBVP gives an extremal which satisfies the necessary conditions of optimality. The MPBVP can be written as a set of non linear equations which are solved by a Newton-like algorithm. This is what we call indirect methods. The sensitivy of Newton algorithms with respect to the initial guess is well known and we use the result from the direct method as starting guess to improve the convergence of the indirect method. Because of the phase constraints, we consider multiple shooting techniques. Each intermediate node represents the junction between two arcs. In addition, the singular perturbation is responsible for numerical difficulties and we need to add nodes on subarcs to improve numerical stability. See [7] for details about simple and multiple shooting methods.

From the numerical point of view, we have to solve a MPBVP with singular perturbation. There exists efficient dedicated methods, see [9]. The main advatange of these methods is that the choice of the mesh is based on local error and conditioning, taking into account the singular perturbation. In this article, we simply fix arbitrarily the number of nodes on each subarcs (between 10 and 16) and we uniformly space them. Between two nodes, we integrate with a variable step-size Runge-Kutta scheme (*radau5*, see [18]), particularly efficient for stiff problems. It would be interesting to compare these two approaches. In this study, we choose to use standard methods in optimal control

DOI: 10.1002/oca

and we want to get benefit from the complementary of direct and indirect methods. We refer to [32] for a short survey of numerical direct and indirect methods for optimal control problems, with an exhaustive list of softwares established in 2009. Many efficient codes exist and we choose two open-source codes, the *Bocop* software [4] for the direct method and the *HamPath* package [8] for the indirect method. One distinctive feature of *HamPath* code is that it is based on the maximized Hamiltonian and the adjoint system is automatically computed by Automatic Differentiation. On the other hand, the user has to give the parameterization of the control and the multilpliers (associated to the state constraints).

The paper is organized as follows. The physical model with the optimal control problem are defined in section 2. We give preliminary numerical results from the direct method at the end of this section. This gives an insight into the optimal structures. In section 3, we analyze the optimal control problem with the application of the maximum principle with phase constraints. Then numerical algorithms and results are presented in section 4. Section 5 concludes the article.

2. PHYSICAL MODEL AND MAYER OPTIMAL CONTROL PROBLEM

2.1. Aircraft performance model

In this section, the aircraft dynamics equation is presented. A non linear point-mass representation is used. An aircraft is subjected to four forces, its own weight $\overrightarrow{P}$, the Lift $\overrightarrow{L}$ which compensate the weight of the aircraft, the Thrust $\overrightarrow{T}$ which we consider colinear to the velocity vector $\overrightarrow{V}$ and the Drag force $\overrightarrow{D}$ which corresponds to friction between the aircraft and the air, see Figure 2.

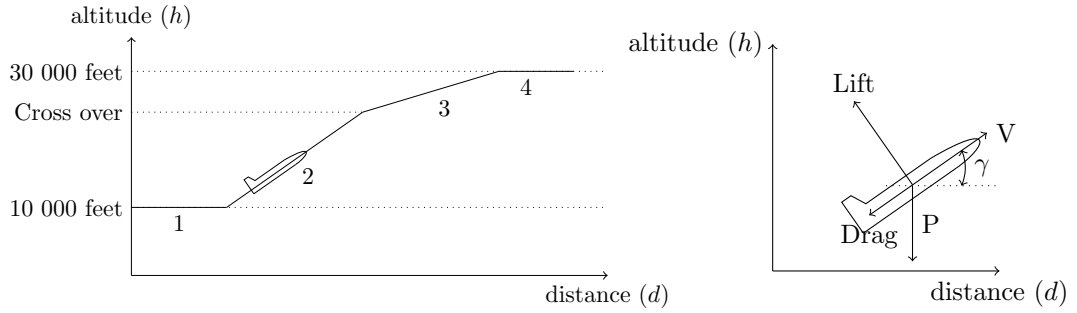

Figure 2. (a): A typical climb procedure, (1) the aircraft increases its speed at constant altitude. (2) Once it reaches its climbing speed, it starts to climb until reaching cross over altitude. (3) after reaching the cross over altitude, the aircraft follows a trajectory at constant mach speed. (4) Finally, the aircraft reaches its cruise altitude. (b): Forces representation. The angle between the Thrust and the velocity vector is ignored.

The first Dynamic Principle provides the equations of motion of this aircraft with respect to t.

$$\begin{aligned}
\frac{\mathrm{d}h}{\mathrm{d}t}(t) &= V(t)\sin(\gamma(t)) \\
\frac{\mathrm{d}d}{\mathrm{d}t}(t) &= V(t)\cos(\gamma(t)) \\
m(t)\frac{\mathrm{d}V}{\mathrm{d}t}(t) &= \varepsilon T_{\max}(h(t)) - \frac{1}{2}\rho(h(t))SV(t)^2C_D(C_L) - m(t)g\sin(\gamma(t)) \\
\frac{\mathrm{d}m}{\mathrm{d}t}(t) &= -\varepsilon C_s(V(t))T_{\max}(h(t)) \\
m(t)V(t)\frac{\mathrm{d}\gamma}{\mathrm{d}t}(t) &= \frac{1}{2}\rho(h(t))SV(t)^2C_L - m(t)g\cos(\gamma(t))
\end{aligned} \tag{1}$$

The description of the parameters is given in Table I. To represent air density ρ, temperature Θ and pressure P as smooth functions of altitude h, we use the smooth *International Standard Atmosphere*

DOI: 10.1002/oca

Parameter	Description	Unit
h	Altitude	m
d	Longitudinal distance	m
V	True air speed	m.s^{-1}
m	Aircraft mass	kg
γ	Air slope	
$T_{\max}$	Maximum thrust	N
C_s	Fuel flow model	kg.N^{-1}.s^{-1}
S	Wing area	m.s^2
ρ	Air density	kg.m^{-3}
g	Gravitational constant (assume to be constant)	m.s^{-2}
C_L	Lift coefficient	
C_D	Drag coefficient	
ε	Ratio of maximum thrust	

Table I. Description of the data from aircraft dynamics.

(ISA) model. In this study, altitude will not be higher than 11 000 meters, so we could restrain ISA model to:

$$\Theta(h) \coloneqq \Theta_0 - \beta h, \quad P(h) \coloneqq P_0 \left(\frac{\Theta(h)}{\Theta_0}\right)^{\frac{g}{\beta R}} \quad \text{and} \quad \rho(h) \coloneqq \frac{P(h)}{R\Theta(h)}.$$

We also use the *BADA* model [30] from EUROCONTROL which provides a general smooth aircraft performance model and specific values of coefficients, depending on the type of the aircraft:

$$\begin{aligned} T_{\max}(h) &\coloneqq C_{T_1}\left(1 - \frac{h}{C_{T_2}} + C_{T_3}h^2\right), \\ C_s(V) &\coloneqq C_{s_1}\left(1 + \frac{V}{C_{s_2}}\right), \\ C_D(C_L) &\coloneqq C_{D_1} + C_{D_2}{C_L}^2. \end{aligned}$$

The description of the parameters from ISA and BADA models is given in Table. II.

Parameter	Description	Unit
P_0	Standard pressure	Pa
Θ_0	Standard temperature	K
R	Perfect gases constant	J.kg^{-1}.K^{-1}
β	Variation of temperature w.r.t altitude	K.m^{-1}
C_{T_1}	Aicraft specific data for thrust	N
C_{T_2}	Aicraft specific data for thrust	m
C_{T_3}	Aicraft specific data for thrust	m^{-2}
C_{s_1}	Aicraft specific data for fuel flow	kg.N^{-1}.s^{-1}
C_{s_2}	Aicraft specific data for fuel flow	m.s^{-1}
C_{D_1}, C_{D_2}	Aircraft specific data for drag	
γ_{air}	Heat capacity ratio of air	
$\mu \coloneqq \frac{\gamma_{\text{air}}-1}{\gamma_{\text{air}}}$	Constant derived from Heat capacity ratio	

Table II. Description of the parameters from ISA and BADA models.

The aircraft evolves in a constrained context: these contraints arise from *air traffic control* (ATC) or physical limitations. In order to protect the structure of the aircraft its speed is limited. As it is

DOI: 10.1002/oca

difficult to compute the real speed, a *Computed Air Speed* (CAS) which is given by a *Pitot tube* is used and limited by the *Operation Maximal Speed* (VMO), see eq. (2). Beyond a given altitude, *Mach* speed is usually used and limited by the *Maximal Mach Operation* (MMO), see eq. (3). Other constraints are coming from ATC. For example, in a climbing phase the aircraft is not allowed to go down ($\gamma \geq 0$) and to avoid the stall of the aircraft the air slope is limited ($\gamma \leqslant \gamma_{\max}$). Only the constraints arising from the air slope and the Mach speed will be taken into account in this study:

$$CAS \coloneqq \sqrt{\frac{2P_0}{\mu\,\rho(0)}\left(\left(\frac{P(h)}{P_0}\left(\left[\frac{\mu V^2}{2R\,\Theta(h)}+1\right]^{\frac{1}{\mu}}-1\right)+1\right)^{\mu}-1\right)} \leqslant VMO, \tag{2}$$

$$M \coloneqq \frac{V}{a(h)} = \frac{V}{\sqrt{\gamma_{\text{air}}\,R\,\Theta(h)}} \leqslant MMO. \tag{3}$$

2.2. Mayer formulation of the optimal control problem

Let note $x \coloneqq (h, d, V, m, \gamma)$ the state, $M \coloneqq \mathbb{R}^5$ the state space, $u \coloneqq (\varepsilon, C_L)$ the control, $U \coloneqq \{u = (u_1, u_2) \in \mathbb{R}^2, u_i \in [u_{i,\min}, u_{i,\max}], i = 1, 2\}$ the control domain. We put all constant data in a vector ω which belongs to $\mathbb{R}^{15}$:

$$\omega \coloneqq \big(S, g, C_{T_1}, C_{T_2}, C_{T_3}, C_{D_1}, C_{D_2}, C_{s_1}, C_{s_2}, R, \Theta_0, \beta, P_0, \mu, \gamma_{\text{air}}\big),$$

with $\omega_i > 0$, $i = 1, \ldots, 15$. The values of the parameters are given in Table III in section 2.3. The dynamics from eq. (1) can be written in the form

$$f(x(t), u(t)) \coloneqq f_0(x(t)) + u_1(t) f_1(x(t)) + u_2(t) f_2(x(t)) + u_2(t)^2 f_3(x(t)),$$

where f_0, f_1, f_2 and f_3 are the following smooth vector fields:

$$\begin{aligned}
f_0(x) &\coloneqq x_3\big(\sin(x_5)\frac{\partial}{\partial x_1} + \cos(x_5)\frac{\partial}{\partial x_2}\big) - \big(\omega_6\,\theta_3(x,\omega) + \omega_2\sin(x_5)\big)\frac{\partial}{\partial x_3} - \frac{\omega_2}{x_3}\cos(x_5)\frac{\partial}{\partial x_5},\\
f_1(x) &\coloneqq \frac{\theta_1(x,\omega)}{x_4}\frac{\partial}{\partial x_3} - \theta_1(x,\omega)\,\theta_2(x,\omega)\frac{\partial}{\partial x_4},\\
f_2(x) &\coloneqq \frac{\theta_3(x,\omega)}{x_3}\frac{\partial}{\partial x_5},\\
f_3(x) &\coloneqq -\omega_7\,\theta_3(x,\omega)\frac{\partial}{\partial x_3},
\end{aligned}$$

and where $\theta(x,\omega) \coloneqq (\theta_1(x,\omega), \theta_2(x,\omega), \theta_3(x,\omega), \theta_4(x,\omega), \theta_5(x,\omega))$ is a vector of auxiliary functions with

$$\begin{aligned}
&\theta_1(x,\omega) \coloneqq \omega_3\left(1 - \frac{x_1}{\omega_4} + \omega_5 x_1^2\right), \quad \theta_2(x,\omega) \coloneqq \omega_8\left(1 + \frac{x_3}{\omega_9}\right), \quad \theta_3(x,\omega) \coloneqq \frac{\omega_1\,x_3^2\,\theta_5}{2\,\omega_{10}\,x_4\,\theta_4},\\
&\theta_4(x,\omega) \coloneqq \omega_{11} - \omega_{12}\,x_1, \quad \theta_5(x,\omega) \coloneqq \omega_{13}\left(\frac{\theta_4}{\omega_{11}}\right)^{\frac{\omega_2}{\omega_{10}\omega_{12}}}.
\end{aligned}$$

The climbing phase starts from the fixed initial state $x_0 \coloneqq (h_0, d_0, V_0, m_0, \gamma_0) \in M$ and stops when the state reaches the terminal submanifold $M_f \coloneqq \{x \in M,\ b(x) = 0\}$, with

$$b(x) \coloneqq \begin{pmatrix} x_1 - x_{1,f} \\ x_2 - x_{2,f} \\ x_3 - x_{3,f} \\ x_5 - x_{5,f} \end{pmatrix},$$

where $x_{1,f}$, $x_{2,f}$, $x_{3,f}$ and $x_{5,f}$ are fixed final conditions. The final mass is free. The state constraints the aircraft has to satisfy all along the trajectory, see subsection 2.1, are put together in a vector of

DOI: 10.1002/oca

constraints c defined by

$$c(x) \coloneqq \begin{pmatrix} x_{5,\min} - x_5 \\ \psi(x) - \psi_{\max} \end{pmatrix}, \quad \text{with} \quad \psi(x) \coloneqq \frac{x_3}{\sqrt{\omega_{15}\,\omega_{10}\,\theta_4(x,\omega)}}.$$

The two main contributors which cost to a company during a flight are the fuel consumption and the flight duration. That is why we are interested in a mixed objective function which combines these two contributors. Finally, the optimal control problem can be summarized this way:

$$(\mathcal{P}_\alpha) \quad \begin{cases} g_\alpha(t_f, x(t_f)) \coloneqq (1-\alpha)\,(x_{0,4} - x_4(t_f)) + \alpha\, t_f \longrightarrow \min\limits_{t_f, u(\cdot)}, \quad \alpha \in [0,1] \text{ fixed}, \\ \dot{x}(t) = f(x(t), u(t)), \quad u(t) \in U, \quad t \in [0, t_f] \textit{ a.e.}, \quad t_f > 0, \quad x(0) = x_0, \\ c_i(x(t)) \leqslant 0, \quad i = 1, 2, \quad t \in [0, t_f], \\ b(x(t_f)) = 0. \end{cases}$$

2.3. Preliminary numerical results

We give in this section some preliminary results on the structures of the trajectories for two different problems: $\alpha = 1$ (minimum time problem) and $\alpha = 0.6$, for a medium-haul aircraft, see Table III. For each problem we compare the strategies for both the state constrained and the state unconstrained cases. In the state unconstrained case, we simply remove the constraints $c_i(x(t)) \leqslant 0$, $i = 1, 2$. We use a direct method within the *Bocop* software, see section 4, to get the following numerical results. The discretisation is realised using a gauss scheme of order 4 with 300 nodes for $\mathcal{P}_1$ and 500 nodes for $\mathcal{P}_{0.6}$. In the unconstrained cases, the initial guesses are set to look like a common climbing profile. The results of the unconstrained problem are then used as the initial guesses for the constrained problems. The following results are obtained with $m_0 = 72\,000$ kg for $(\mathcal{P}_1)$ and with $m_0 = 59\,000$ kg for $(\mathcal{P}_{0.6})$.

On Figure 3 (resp. 4), we display the values of the constraints and the controls along the trajectories solution of problem $(\mathcal{P}_1)$ (resp. $(\mathcal{P}_{0.6})$) for both cases: with and without taking into account the state constraints. We can see that the constraint on the air slope $c_\gamma(x) \coloneqq x_{5,\min} - x_5(x)$ is necessary for both problems whereas the constraint on the Mach speed $c_v(x) \coloneqq \psi(x) - \psi_{\max}$ comes up only in problem $(\mathcal{P}_{0.6})$. Note that these two constraints are not active simultaneously.

Remark 1. In this paper, we restrict the theoretical study to the observations from this section.

3. ANALYSIS OF PROBLEM $(\mathcal{P}_\alpha)$ WITH MAXIMUM PRINCIPLE WITH PHASE CONSTRAINTS

3.1. Preliminary remarks

The necessary optimality conditions we are interested in are given by the *maximum principle* with state constraints [19, 22, 23, 31] . There are two approaches to get necessary optimality conditions: direct or indirect adjoining. Assuming we have only one single state constraint, in the direct adjoining method, this state constraint is directly adjoined to the Hamiltonian while in the indirect approach, the derivative of the constraint is adjoined. In this article, we consider the direct adjoining method since in this case, we have a direct link between the direct and indirect numerical methods. Indeed, in the indirect method (*i.e.* shooting method), the discretization of the parameterized multiplier associated to the state constraint gives (under some assumptions) the multipliers of the discretized optimal control problem associated to the discrete state constraints, see proposition 4.1 and Figure 6.

Another important remark is the following. According to [19], the maximum principle (in its general setting) which is commonly used when dealing with optimal control problems with state constraints has no rigorous proof in the literature. In [19], this maximum principle is referred as an

DOI: 10.1002/oca

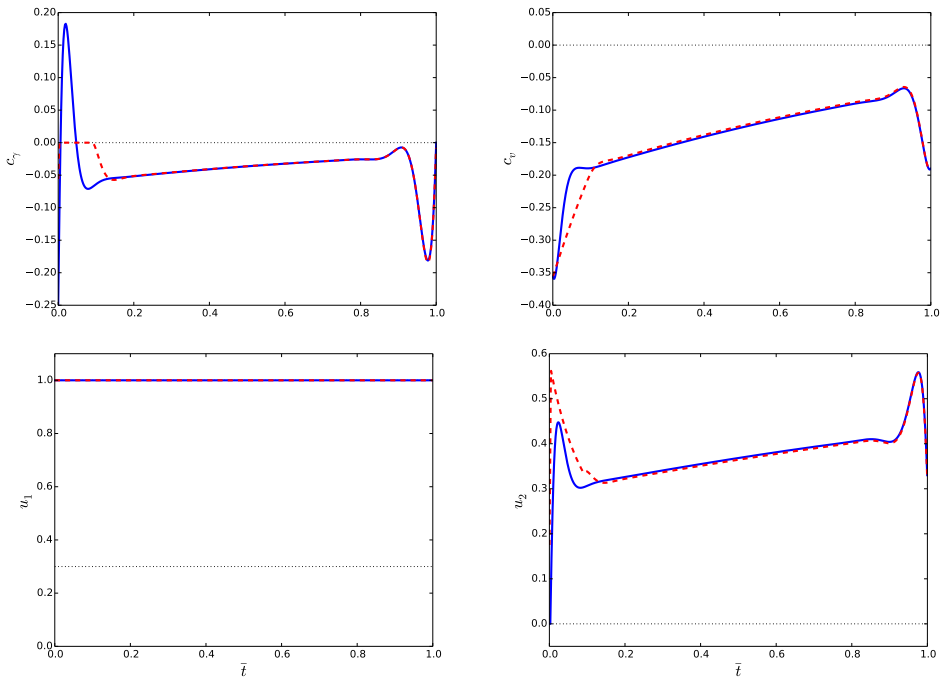

Figure 3. Evolution of the constraints and the controls along a time minimum trajectory ($\alpha = 1$) with respect to the normalized time $\bar{t}$. The red dashed lines represent problem $(\mathcal{P}_1)$ while the same problem without state constraints is represented by blue solid lines. The boundaries of state and control constraints are given by the dotted horizontal lines.

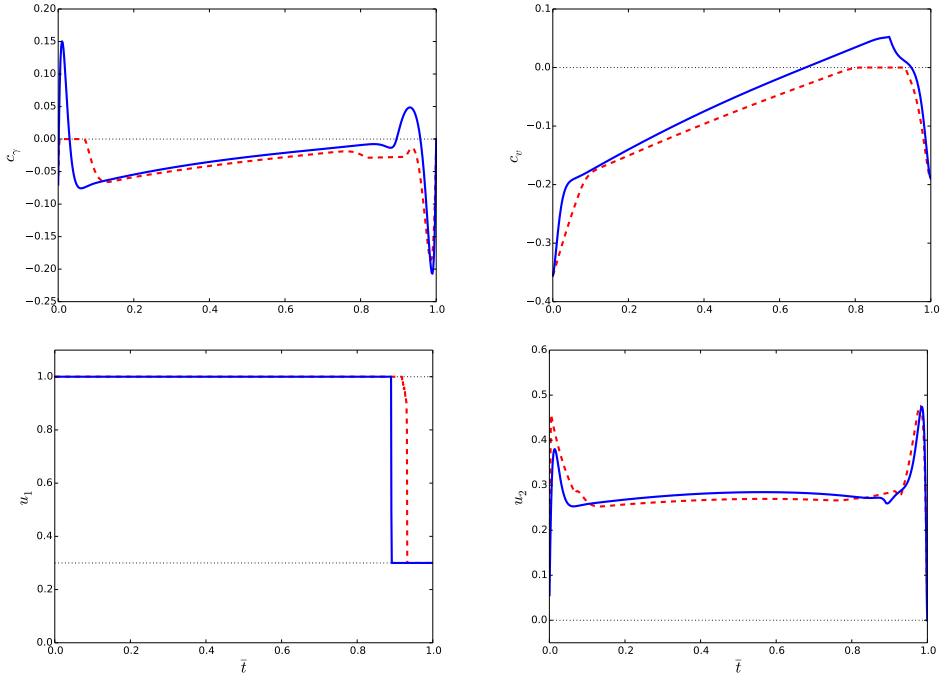

Figure 4. Evolution of the constraints and the controls along a time minimum trajectory ($\alpha = 0.6$) with respect to the normalized time $\bar{t}$. The red dashed lines represent problem $(\mathcal{P}_{0.6})$ while the same problem without state constraints is represented by blue solid lines. The boundaries of state and control constraints are given by the dotted horizontal lines.

DOI: 10.1002/oca

Parameter	Value	Parameter	Value
ω_1	122.6	$x_{1,0}$	3480
ω_2	9.81	$x_{2,0}$	0
ω_3	141040	$x_{3,0}$	151.67
ω_4	14909.9	$x_{4,0}$	$\in [4.8 \times 10^4, 7.6 \times 10^4]$
ω_5	6.997×10^{-10}	$x_{5,0}$	0.07
ω_6	0.0242	$x_{1,\mathrm{f}}$	9144
ω_7	0.0469	$x_{2,\mathrm{f}}$	150 000
ω_8	1.055×10^{-5}	$x_{3,\mathrm{f}}$	191.0
ω_9	441.54	$x_{5,\mathrm{f}}$	0
ω_{10}	287.058	$\psi_{\max}$	0.82
ω_{11}	288.15	$x_{5,\min}$	0
ω_{12}	0.0065	$u_{1,\min}$	0.3
ω_{13}	101325	$u_{2,\min}$	0
ω_{14}	0.2857	$u_{1,\max}$	1
ω_{15}	1.4	$u_{2,\max}$	1.6

Table III. Values of the constant parameters.

informal theorem. The author gives a more abstract version of this result which is a theorem but which is not suited for practical purposes. One difficulty is to guarantee the absence of a singular part in the adjoint vector and the multiplier associated to the state constraint which are functions of bounded variation. To avoid this ill-behaviour, we consider only trajectories with finitely many junction[†] times with the constraint and we look for piecewise smooth optimal control. We assume also that the initial and final times are not junction times.

3.2. Necessary optimality conditions

Let define the pseudo-Hamiltonian of the *Mayer* optimal control problem ($\mathcal{P}_\alpha$) by

$$\begin{aligned} H \colon T^*M \times U \times \mathbb{R}^2 &\longrightarrow \mathbb{R} \\ (x, p, u, \eta) &\longmapsto H(x, p, u, \eta) \coloneqq \langle p, f(x, u)\rangle + \langle \eta, c(x)\rangle \end{aligned}$$

where T^*M is the cotangent bundle of M and η is the Lagrange multiplier associated to the constraint vector $c(x)$. If $(u^*(\cdot), t_f^*)$ is optimal with $x^*(\cdot)$ the associated optimal trajectory, then assuming $u^*(\cdot)$ is piecewise smooth, $x^*(\cdot)$ has finitely many junction times with the constraint, and assuming the final time is not a junction time, then the maximum principle asserts that there exists a real number $p^0 \leqslant 0$ and a piecewise absolutely continuous costate trajectory $p^*(\cdot)$ such that $(p^*(\cdot), p^0)$ does not vanish on $[0, t_f^*]$. Besides, there exists a function $\eta^*(\cdot)$ such that $\eta_i^*(t) \leqslant 0$ and $\eta_i^*(t)\, c_i(x^*(t)) = 0$, $i = 1, 2$, for all t in $[0, t_f^*]$. Moreover, we have for almost every $t \in [0, t_f^*]$

$$\dot{x}^*(t) = \frac{\partial H}{\partial p}(x^*(t), p^*(t), u^*(t), \eta^*(t)), \quad \dot{p}^*(t) = -\frac{\partial H}{\partial x}(x^*(t), p^*(t), u^*(t), \eta^*(t)) \tag{4}$$

and we have the maximization condition

$$H(x^*(t), p^*(t), u^*(t), \eta^*(t)) = \max_{u \in U} H(x^*(t), p^*(t), u, \eta^*(t)). \tag{5}$$

The boundary conditions must be fulfilled and we have the following transversality conditions:

$$p^*(t_f^*) = p^0 \frac{\partial g_\alpha}{\partial x}(t_f^*, x^*(t_f^*)) + \sum_{k=1}^{4} \lambda_k\, b_k^{'}(x^*(t_f^*)), \quad (\lambda_1, \ldots, \lambda_4) \in \mathbb{R}^4 \tag{6}$$

[†]A junction time is either an entry or an exit time of a boundary arc. A contact time is a time when the arc has an isolated contact with the boundary.

DOI: 10.1002/oca

Since the final time t_f^* is free, if $u^*(\cdot)$ is continuous at time t_f^*, we have:

$$H[t_f^*] = -p^0 \frac{\partial g_\alpha}{\partial t}(t_f^*, x^*(t_f^*)), \tag{7}$$

where $[t]$ stands for $(x^*(t), p^*(t), u^*(t), \eta^*(t))$. Let $\mathcal{T}$ denote the finite set of contact and junction times with the boundary. Then at $\tau \in \mathcal{T}$ we have

$$H[\tau^+] = H[\tau^-], \tag{8}$$

$$p(\tau^+) = p(\tau^-) - \nu_{i,\tau}\, c_i'(x(\tau)), \quad \nu_{i,\tau} \leqslant 0, \quad i = 1, 2. \tag{9}$$

Remark 2. Either $p^0 = 0$ (*abnormal case*), or p^0 can be set to -1 by homogeneity (*normal case*). We consider only the normal case.

Definition 1. We call an *extremal* the quadruplet $(x(\cdot), p(\cdot), u(\cdot), \eta(\cdot))$ defined on $[0, t_f]$ where $u(\cdot)$ is an admissible control[‡] and which satisfies eqs. (4), (5), (8), (9). Any extremal satisfying the boundary conditions and equations (6), (7) is called a *BC-extremal*. We define the *Hamiltonian lifts* $H_i(z) \coloneqq \langle p, f_i(x)\rangle,\ i = 1, \ldots, 4,\ z \coloneqq (x, p)$, and the function $\varphi(t) \coloneqq \frac{\partial H}{\partial u}(z(t), u(t), \eta(t)) = (\varphi_1(t), \varphi_2(t))$, with $\varphi_1(t) = H_1(z(t))$ and $\varphi_2(t) = H_2(z(t)) + 2\, u_2(t)\, H_3(z(t))$.

3.3. Adjoint equations and transversality conditions

Using conditions (4), we get the adjoint equations[§]:

$$\begin{aligned}
\dot{p}_1 &= p_3 \frac{\theta_3}{\theta_4}(\omega_{12} - \frac{\omega_2}{\omega_{10}})(\omega_6 + u_2^2\omega_7) - u_1\omega_3(\frac{p_3}{x_4} - p_4\theta_2)(-\frac{1}{\omega_4} + 2\omega_5 x_1) \\
&\quad - p_5 \frac{u_2}{x_3}\frac{\theta_3}{\theta_4}(\omega_{12} - \frac{\omega_2}{\omega_{10}}) - \langle \eta, \frac{\partial c}{\partial x_1}\rangle, \\
\dot{p}_2 &= 0, \\
\dot{p}_3 &= -p_1 \sin(x_5) - p_2 \cos(x_5) + 2p_3 \frac{\theta_3}{x_3}\left(\omega_6 + u_2^2\omega_7\right) + p_4\theta_1 \frac{\omega_8}{\omega_9} u_1 \\
&\quad - \frac{p_5}{x_3^2}\left(u_2\theta_3 + \omega_2 \cos(x_5)\right) - \langle \eta, \frac{\partial c}{\partial x_3}\rangle, \\
\dot{p}_4 &= -p_3 \frac{\theta_3}{x_4}\left(\omega_6 + \omega_7 u_2^2\right) + p_3 \frac{\theta_1}{x_4^2} u_1 + p_5 \frac{\theta_3}{x_3 x_4} u_2 - \langle \eta, \frac{\partial c}{\partial x_4}\rangle, \\
\dot{p}_5 &= x_3(-p_1 \cos(x_5) + p_2 \sin(x_5)) + p_3\omega_2 \cos(x_5) - p_5 \frac{\omega_2}{x_3} \sin(x_5) - \langle \eta, \frac{\partial c}{\partial x_5}\rangle.
\end{aligned} \tag{10}$$

From equations (6) and (7) we have $p_4^*(t_f^*) = p^0(\alpha - 1)$ and $H[t_f^*] = -p^0\alpha$. Since the system is autonomous, the Hamiltonian is constant along any extremal and then $H[t] = -p^0\alpha$, $t \in [0, t_f]$ *a.e.*

3.4. Lie bracket configuration

3.4.1. Notation

If f is a smooth function on M and X is a smooth vector field on M, X acts on f by the *Lie derivative* $f \mapsto X \cdot f$ with $(X \cdot f)(x) \coloneqq f'(x)X(x)$. Considering two smooth vector fields X_0 and X_1, the operator $X_1 \mapsto [X_0, X_1] \coloneqq X_0 \cdot X_1 - X_1 \cdot X_0$ gives the *Lie bracket* on vector fields. The *Poisson bracket* of the two Hamiltonian lifts H_0 and H_1 of X_0 and X_1 is defined by $\{H_0, H_1\} \coloneqq \overrightarrow{H}_0 \cdot H_1$ where $\overrightarrow{H}_0 \coloneqq (\partial_p H_0, -\partial_x H_0)$. We use the notation H_{01} (resp. X_{01}) to denote the bracket $\{H_0, H_1\}$ (resp. $[X_0, X_1]$). Since H_0 and H_1 are two Hamiltonian lifts, $\{H_0, H_1\} = \langle p, [X_0, X_1]\rangle$.

[‡]An admissible control is a L^∞-mappings on $[0, t_f]$ taking its values in U such that the associated trajectory $x(\cdot)$ is globally defined on $[0, t_f]$.
[§]If necessary, we omit arguments of the functions for readibility.

DOI: 10.1002/oca

3.4.2. Computations of Lie brackets

Let introduce the vector field

$$f_{02}(x) = -\theta_3 \cos(x_5)\frac{\partial}{\partial x_1} + \theta_3 \sin(x_5)\frac{\partial}{\partial x_2} + \frac{\omega_2\theta_3}{x_3}\cos(x_5)\frac{\partial}{\partial x_3} + \left(\frac{\theta_3}{\theta_4}\left(\omega_{12} - \frac{\omega_2}{\omega_{10}}\right)\sin(x_5) - \frac{\theta_3}{x_3^2}\left(\omega_6\theta_3 + 2\omega_2\sin(x_5)\right)\right)\frac{\partial}{\partial x_5},$$

then we have the following proposition.

Proposition 3.1. *The vector set* $(f_0(x), f_1(x), f_2(x), f_3(x), f_{20}(x))$ *forms a basis of* T_xM *for every* $x \in M_1 \coloneqq \{x \in M,\, x_1 \neq \frac{\omega_{11}}{\omega_{12}},\, x_1 \neq \frac{1\pm\sqrt{1-4\omega_4^2\omega_5}}{2\omega_4\omega_5},\, x_3 \neq 0,\, x_3 \neq -\omega_9,\, x_4 \neq 0\}$.

Proof
We have $\det\left(f_0(x), f_1(x), f_2(x), f_3(x), f_{02}(x)\right) = -\omega_7\theta_1\theta_2\theta_3^3 \neq 0$ for $x \in M_1$. □

In our problem, quantities θ_1, θ_2 and θ_3 could not be equal to zero due to physical considerations, so any trajectory $x(\cdot)$ belongs to M_1 and we can express all the Lie brackets on the basis previously defined. Brackets of order two are then:

$$f_{01} = a_{01}f_0 + b_{01}f_1 + d_{01}f_2 + e_{01}f_3, \quad f_{03} = a_{03}f_0 + d_{03}f_2 + e_{03}f_3,$$
$$f_{21} = d_{21}f_2, \quad f_{31} = b_{31}f_1 + e_{31}f_3, \quad f_{23} = d_{23}f_2,$$

where

- $a_{01} = -\dfrac{\theta_1}{x_3x_4}$,
- $b_{01} = \omega_3\dfrac{x_3}{\theta_1}\left(-\dfrac{1}{\omega_4} + 2\omega_5x_1\right)\sin(x_5) - \dfrac{1}{\theta_2}\dfrac{\omega_8}{\omega_9}\left(\omega_6\theta_3 + \omega_2\sin(x_5)\right)$,
- $d_{01} = -\dfrac{2}{x_3x_4}\dfrac{\theta_1}{\theta_3}\omega_2\cos(x_5)$,
- $e_{01} = -2\dfrac{\theta_1}{x_3x_4}\dfrac{\omega_6}{\omega_7} - \dfrac{\theta_1\theta_2}{x_4}\dfrac{\omega_6}{\omega_7} + \dfrac{1}{\omega_7}\dfrac{\theta_1}{\theta_3x_4}\left(\omega_6\theta_3 + \omega_2\sin(x_5)\right)\left(\dfrac{1}{x_3} - \dfrac{\omega_8}{\omega_9\theta_2}\right)$,
- $a_{03} = \omega_7\dfrac{\theta_3}{x_3}$,
- $d_{03} = 2\dfrac{\omega_2\omega_7}{x_3}\cos(x_5)$,
- $e_{03} = -\omega_6\dfrac{\theta_3}{x_3} + \left(\dfrac{x_3}{\theta_4}\left(\omega_{12} - \dfrac{\omega_2}{\omega_{10}}\right) - 3\dfrac{\omega_2}{x_3}\right)\sin(x_5)$,
- $d_{21} = -\dfrac{\theta_1}{x_4}\left(\dfrac{1}{x_3} + \theta_2\right)$,
- $b_{31} = -\dfrac{\omega_7\omega_8}{\omega_9}\dfrac{\theta_3}{\theta_2}$,
- $e_{31} = -\dfrac{\theta_1}{x_4}\left(\theta_2 + \dfrac{2}{x_3} + \dfrac{\omega_8}{\omega_9\theta_2}\right)$,
- $d_{23} = \omega_7\dfrac{\theta_3}{x_3}$.

3.5. Parameterization of extremal curves (state unconstrained case)

Let consider first the state unconstrained case. We denote by $\bar{u}_2(z) \coloneqq -H_2(z)/2H_3(z)$, the value that cancels φ_2. Hence the controls that maximize the Hamiltonian are given by:

$$u_1(z) = \begin{cases} u_{1,\max}, \text{ if } H_1(z) > 0, \\ u_{1,\min}, \text{ if } H_1(z) < 0, \\ u_{1,s}(z) \in [u_{1,\min}, u_{1,\max}], \text{ if } H_1(z) = 0, \end{cases}$$

DOI: 10.1002/oca

and

- if $H_3(z) > 0$, then $u_2(z) = \arg\max(H(u_{2,\min}), H(u_{2,\max}))$,
- if $H_3(z) < 0$, then $u_2(z) = \begin{cases} u_{2,\max}, \text{ if } \bar{u}_2(z) > u_{2,\max}, \\ u_{2,\min}, \text{ if } \bar{u}_2(z) < u_{2,\min}, \\ \bar{u}_2(z), \text{ if } \bar{u}_2(z) \in [u_{2,\min}, u_{2,\max}], \end{cases}$
- if $H_3(z) = 0$, then $u_2(z) = \begin{cases} u_{2,\max}, \text{ if } H_2(z) > 0, \\ u_{2,\min}, \text{ if } H_2(z) < 0, \\ u_{2,s}(z) \in [u_{2,\min}, u_{2,\max}], \text{ if } H_2(z) = 0. \end{cases}$

Along any extremal, if the control $u(\cdot)$ belongs to the interior of the control domain U then the *Legendre-Clebsch* condition

$$\frac{\partial^2 H}{\partial u^2}(z(t), u(t), \eta(t))(v, v) \leqslant 0, \quad \forall v \in \mathbb{R}^2, \quad \forall t \in [0, t_f],$$

must be satisfied, *i.e.* $H_3(z(t)) \leqslant 0$ for all t in $[0, t_f]$.

3.6. Computations of controls, multipliers and junction conditions (one state constraint)

We only analyze cases we encounter in the numerical experiments. Hence, we focus our study on a scalar state constraint c. We call η its associated multiplier.

Definition 2. A *boundary arc* associated to a state constraint c, is an arc $\gamma_c \colon t \mapsto \gamma_c(t)$ defined on an interval $J = [t_1, t_2]$, not reduced to a singleton, such that $c(\gamma_c(t)) = 0$ for all t in J.

Definition 3. We define the order m of the constraint c as the first integer such that a control variable appear after the m-th differentiation of c with respect to time.

3.6.1. General results

Lemma 3.2. *The state constraints c_γ and c_v are of order 1.*

Proof
The derivative of ψ is

$$\dot{\psi} = \frac{\partial \psi}{\partial x_1}\dot{x}_1 + \frac{\partial \psi}{\partial x_3}\dot{x}_3 = \frac{\partial \psi}{\partial x_1}\dot{x}_1 + \frac{\partial \psi}{\partial x_3}\left(-\omega_6\theta_3 - \omega_2 \sin(x_5) + u_1\frac{\theta_1}{x_4} - u_2^2\omega_7\theta_3\right) \tag{11}$$

and so $c_v = \psi - \psi_{\max}$ is of order 1. Since $\dot{c}_\gamma = \dot{x}_5 = -\frac{\omega_2}{x_3}\cos(x_5) + u_2\frac{\theta_3(x,\omega)}{x_3}$, c_γ is of order 1. □

Lemma 3.3. *The partial derivatives of ψ are equal to:*

$$\frac{\partial \psi}{\partial x_1}(x) = \frac{x_3\omega_{12}}{\theta_4\sqrt{\omega_{10}\omega_{12}\theta_4}} = \frac{\omega_{12}}{2\theta_4}\psi(x) \quad \textit{and} \quad \frac{\partial \psi}{\partial x_3}(x) = \frac{1}{\sqrt{\omega_{10}\omega_{12}\theta_4}} = \frac{\psi(x)}{x_3}.$$

We present now the general framework used to parameterize extremals with state constraints c of order 1. Since c is of order 1, we could write in a generic way, $\dot{c} = a_0 + u_1 a_1 + u_2 a_2 + u_2^2 a_3$ with $(a_1, a_2, a_3) \neq (0, 0, 0)$ and with a_0, a_1, a_2 and a_3 depending on x.

Lemma 3.4. *Along the boundary, $\{H, H_i\} = H_{0i} + u_1 H_{1i} + u_2 H_{2i} + u_2^2 H_{3i} - \eta c' f_i$, $i = 0, \ldots, 3$.*

Proof
Computing, $\{H, H_i\} = H_{0i} + u_1 H_{1i} + u_2 H_{2i} + u_2^2 H_{3i} + \{\eta c, H_i\}$, with $\{\eta c, H_i\} = c\{\eta, H_i\} - \eta c' f_i = -\eta c' f_i$ as $c = 0$ and $\frac{\partial c}{\partial p} = 0$. □

Lemma 3.5. *Let consider f_ν a smooth vector field, $H_\nu = \langle p, f_\nu \rangle$ its Hamiltonian lift and τ a junction time. Then we have $\nu_\tau c'(x(\tau)) f_\nu(x(\tau)) = H_\nu(z(\tau^-)) - H_\nu(z(\tau^+))$ at the junction point.*

DOI: 10.1002/oca

Proof
From eq. (9), we have $p(\tau^+) = p(\tau^-) - \nu_\tau c'(x(\tau))$ at the junction time τ. Multiplying by f_ν leads to $H_\nu(z(\tau^+)) = H_\nu(z(\tau^-)) - \nu_\tau c'(x(\tau)) f_\nu(x(\tau))$. □

Lemma 3.6. *Let assume that $\varphi_1 > 0$ and $\varphi_2 = 0$ holds along the boundary arc. Then we have:*

1. *if $(a_2, a_3) = (a_2, 0)$ with $a_2 \neq 0$ then the control $u(x)$ is given by*
$$u(x) = \left(u_{1,\max}, -\frac{a_0 + u_{1,\max} a_1}{a_2} \right).$$
2. *if $(a_2, a_3) = (0, a_3)$ with $a_3 \neq 0$ and $a_3(a_0 + u_{1,\max} a_1) < 0$ then the control $u(x)$ is given by*
$$u(x) = \left(u_{1,\max}, \sqrt{-\frac{a_0 + u_{1,\max} a_1}{a_3}} \right).$$

And in both cases, the multiplier η associated to the constraint c is defined by

$$\eta = \frac{1}{c'(f_2 + 2u_2 f_3)} \left(H_{02} + u_{1,\max}(H_{12} + 2u_2 H_{13}) + 2u_2 H_{03} + u_2^2 H_{23} + 2H_3 u_2' f \right).$$

Proof
Since $\varphi_1 > 0$, $u_1 = u_{1,\max}$. Along the boundary $\dot{c} = a_0 + u_{1,\max} a_1 + u_2 a_2 + u_2^2 a_3 = 0$, $u_2 \geqslant 0$, and we determine u_2 in feedback form by solving this equation. Differentiating φ_2 with respect to time and with lemma 3.4, we have along the boundary arc

$$\dot{\varphi}_2 = H_{02} + u_{1,\max}(H_{12} + 2u_2 H_{13}) + 2u_2 H_{03} + u_2^2 H_{23} + 2H_3 u_2' f - \eta c'(f_2 + 2u_2 f_3) = 0.$$

Since c is of order 1, $c'(f_2 + 2u_2 f_3)$ never vanishes along the boundary arc, whence the result. □

Remark 3. If $\varphi_1 < 0$, then replace $u_{1,\max}$ by $u_{1,\min}$ in lemma 3.6.

Let define now the Hamiltonian $\bar{H}$ depending only on the scalar control u_2 (u_1 is fixed):

$$\bar{H}(x, p, u_2, \eta) \coloneqq H(x, p, (u_{1,\max}, u_2), \eta) = \bar{H}_0 + u_2 H_2 + u_2^2 H_3 + \eta c,$$

where $\bar{H}_0 = H_0 + u_{1,\max} H_1$. The following lemma is due to [5, proposition 2.5].

Lemma 3.7. *Let $(x(\cdot), p(\cdot), u_2(\cdot), \eta(\cdot))$ denote an extremal associated to $\bar{H}$ defined on $[0, t_f]$, satisfying $\frac{\partial \bar{H}}{\partial u_2}(x(t), p(t), u_2(t), \eta(t)) = 0$, $t \in [0, t_f]$, and assume that:*

- *$\exists \alpha > 0$, $\dfrac{\partial^2 \bar{H}}{\partial^2 u_2}(x(t), p(t), u_2(t), \eta(t)) < \alpha$ a.e. on $[0, t_f]$ (strict Legendre-Clebsch condition).*
- *the constraint c is of order 1 and $\exists \beta > 0$, $\left|\dfrac{\partial \dot{c}}{\partial u_2}(x(t), u_2(t))\right| \geqslant \beta$, $\forall t \in [0, t_f]$.*
- *the trajectory has a finite set of junction times.*

Then u_2 is continuous over $[0, t_f]$ and $\nu_\tau = 0$.

3.6.2. Application to problem ($\mathcal{P}_\alpha$)

Extremals in $\mathcal{C}_\gamma = \{x \in M,\ c_\gamma(x) = 0,\ c_v(x) \neq 0\}$. Under assumptions from lemma 3.6, since $\dot{c}_\gamma = \frac{\omega_2}{x_3}\cos(x_5) - u_2 \frac{\theta_3}{x_3}$ with $\frac{\theta_3}{x_3} \neq 0$, we have

$$u_1 = \begin{cases} u_{1,\max}, \text{ if } \varphi_1 > 0, \\ u_{1,\min}, \text{ if } \varphi_1 < 0, \end{cases}$$

$$u_{2,\gamma} \coloneqq \frac{\omega_2}{\theta_3}\cos(x_{5,\min}),$$

$$\eta_\gamma \coloneqq -\frac{x_3}{\theta_3}\left(H_{02} + u_1(H_{12} + 2u_2 H_{13}) + 2u_2 H_{03} + u_2^2 H_{23} + 2H_3 u_2' f \right),$$

$$\nu_\tau = -\frac{\varphi_2(\tau^-) x_3}{\theta_3} \text{ at the entry point, } \nu_\tau = \frac{\varphi_2(\tau^+) x_3}{\theta_3} \text{ at the exit point.}$$

DOI: 10.1002/oca

Extremals in $\mathcal{C}_v = \{x \in M,\ c_\gamma(x) \neq 0,\ c_v(x) = 0\}$. Under assumptions from lemma 3.6, since $\dot{c}_v = \dot{\psi}$ with $\frac{\omega_7\theta_3}{x_3}\psi(x) \neq 0$, we have

$$u_1 = \begin{cases} u_{1,\max}, \text{ if } \varphi_1 > 0, \\ u_{1,\min}, \text{ if } \varphi_1 < 0, \end{cases}$$

$$u_{2,v} \coloneqq \sqrt{\frac{1}{\omega_7\theta_3}\left(\left(\frac{x_3^2\omega_{12}}{2\theta_4} - \omega_2\right)\sin(x_5) - \omega_6\theta_3 + u_1\frac{\theta_1}{x_4}\right)},$$

$$\eta_v \coloneqq -\frac{1}{2u_2\omega_7\theta_3\frac{\partial\psi}{\partial x_3}}\left(H_{02} + u_1\left(H_{12} + 2u_2H_{13}\right) + 2u_2H_{03} + u_2^2H_{23} + 2u_2'fH_3\right),$$

$$\nu_\tau = -\frac{\varphi_2(\tau^-)}{2u_2\omega_7\theta_3\frac{\partial\psi}{\partial x_3}} \text{ at the entry point, } \nu_\tau = \frac{\varphi_2(\tau^+)}{2u_2\omega_7\theta_3\frac{\partial\psi}{\partial x_3}} \text{ at the exit point.}$$

4. NUMERICAL METHODS AND RESULTS

In this section, we present the numerical methods used to solve problem $(\mathcal{P}_\alpha)$. Two different types of techniques are used in this study, direct and indirect approaches. The indirect methods are implemented within the *HamPath* package [8]. Since the optimal control is piecewise smooth, multiple shooting technique [7] is necessary to concatenate the different smooth arcs and moreover on each smooth arc, we need to add intermediate nodes to improve numerical stability arising from the singular perturbation. Direct methods [3, 14], within the *Bocop* software [4], are used first to determine the structure of the BC-extremal (see definition 1) and then to initialize the multiple shooting method.

The *Bocop* software tranforms an infinite dimensional optimal control problem (OCP) into a finite dimensional optimization problem called Non Linear Problem (NLP). Full time discretization is applied to state and control variables. These techniques are generally less precise than indirect methods, but there are more robust with respect to initialization and may be used to determine the optimal structure. The discretized problem from *Bocop* is solved using the interior point solver *Ipopt* [34] with *MUMPS* [1] and all the derivatives are computed using automatic differentiation with *ADOL-C* software [35]. For the multiple shooting problem solved by *HamPath*, the Fortran hybrid Newton method *hybrj* [27] is used to solve the non linear system and all the derivatives are computed using automatic differentiation with *tapenade* software [20].

4.1. Numerical methods

4.1.1. A link between KKT conditions and the maximum principle with state constraints

The optimal control problem is transformed into a fixed final time one ($t = s\,t_f$, $s \in [0,1]$):

$$(\mathcal{P}_\alpha)\begin{cases} \min g(t_f(1), x(1)) \\ \dot{x}(s) = t_f(s)\,f(x(s), u(s)) \\ \dot{t}_f(s) = 0 \\ x(0) = x_0 \ \text{ fixed} \\ c(x(s)) \leqslant 0 \\ c_u(u(s)) = (u_1(s) - u_{1,\max},\ -u_1(s) + u_{1,\min},\ u_2(s) - u_{2,\max},\ -u_2(s) + u_{2,\max}) \leqslant 0. \\ b(x(1)) = 0 \end{cases}$$

The Hamiltonian associated to this optimal control problem is then

$$H(x, t_f, u, p, p_{t_f}, \eta) = \langle t_f\,f(x,u), p\rangle + \langle \eta, c(x)\rangle,$$

and the Lagrangian associated to the Non Linear Problem (NLP) obtained by the discretization of the state equation by implicit Euler scheme is using the notation here $x = (x_1, \ldots, x_N)$, $u =$

DOI: 10.1002/oca

$(u_1, \dots, u_N)$, $p = (p_0, \dots, p_{N-1})$, $\mu = (\mu_1, \dots, \mu_N)$ and $\tilde{\eta} = (\tilde{\eta}_1, \dots, \tilde{\eta}_N)$

$$\begin{aligned} L(x, t_f, u, p, \mu, \tilde{\eta}, \lambda) = \; & g(t_f, x_N) + \sum_{i=0}^{N-1} \langle p_i, x_{i+1} - x_i - h t_f f(x_{i+1}, u_{i+1}) \rangle \\ & + \sum_{i=1}^{N} \langle \mu_i, c_u(u_i) \rangle + \sum_{i=1}^{N} \langle \tilde{\eta}_i, c(x_i) \rangle + \langle \lambda, b(x_N) \rangle. \end{aligned}$$

We have then the following proposition.

Proposition 4.1. *If the maximization of the Hamiltonian is equivalent to its Karush-Kuhn-Tucker conditions and furnishes us the optimal control as a function of the state and adjoint state $u(x, t_f, p)$, then the (KKT) necessary conditions of the (NLP) problem are equivalent to*

1. *The discretization of the adjoint state equation by explicit Euler scheme*

$$\begin{aligned} p_i &= p_{i-1} - h \frac{\partial H}{\partial x}(x_i, t_{f,i}, u_i, p_{i-1}, p_{t_f,i-1}, \eta_i) + \eta_i c'(x_i), \; (\eta_i \coloneqq \tilde{\eta}_i h) \\ p_{t_f,i} &= p_{t_f,i-1} - h \langle f(x_i, u_i), p_{i-1} \rangle. \end{aligned}$$

2. *The maximization of the Hamiltonian*

$$\begin{cases} \max H(x_i, t_f, u_i, p_{i-1}, p_{t_f,i-1}, \eta_i) \\ c_u(u_i) \leqslant 0. \end{cases}$$

3. *The transversality conditions*

$$\begin{aligned} p_N &= -\frac{\partial g}{\partial x}(t_f, x_N) - \lambda b'(x_N) \\ p_{t_f,N} &= -\frac{\partial g}{\partial t_f}(t_f, x_N). \end{aligned}$$

4. $c(x_i) \leqslant 0$, $\eta_i \leqslant 0$, $\langle \eta_i, c(x_i) \rangle = 0 \;\; for \;\; i = 1, \dots, N$
5. $b(x_N) = 0$.

Proof
For the adjoint equation and the transversality conditions the result immediately follows from

$$\frac{\partial L}{\partial x_i}(x, t_f, u, p, \mu, \tilde{\eta}, \lambda) = 0 \;\; \text{and} \;\; \frac{\partial L}{\partial t_f}(x, t_f, u, p, \mu, \tilde{\eta}, \lambda) = 0.$$

For the maximization of the Hamiltonian we compute

$$\frac{\partial L}{\partial u_i}(x, t_f, u, p, \mu, \tilde{\eta}, \lambda) = -h\, t_f \frac{\partial f}{\partial u}(x_i, u_i) p_{i-1} + c'_u(u_i) \mu_i = 0 \;\; \text{for} \;\; i = 1, \dots, N.$$

Then, if we add the conditions $c_u(u_i) \leqslant 0$, $\mu_i \leqslant 0$ and $\langle \mu_i, c_u(u_i) \rangle = 0$, we recognize the (KKT) conditions of the maximization of the Hamiltonian. □

Remark 4. In the unconstrained case and if we don't have constraints on the control, this result is well known [6, 11, 12, 16, 24] and the scheme Figure 5 commutes. A similar result (known as the Covector mapping principle) exists in the case of pseudospectral methods, see [13, 33].

Remark 5. An important point is here that if we want to compute the optimal control from the state and adjoint state variables, we have to compute $u(x_i, p_{i-1})$ and not $u(x_i, p_i)$. See also Figure 6 to observe the difference between the Lagrange multipliers associated to the state constraint in the two cases: KKT on the NLP problem and discretization of the BVP problem.

DOI: 10.1002/oca

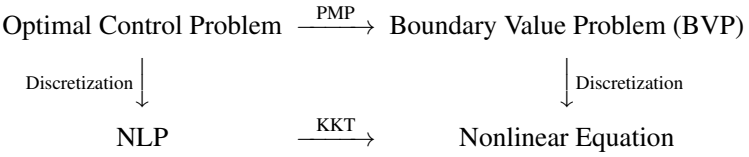

Figure 5. *This scheme commutes if the discretization of the state-adjoint state equation is a partitioned Runge-Kutta and symplectic scheme [17].*

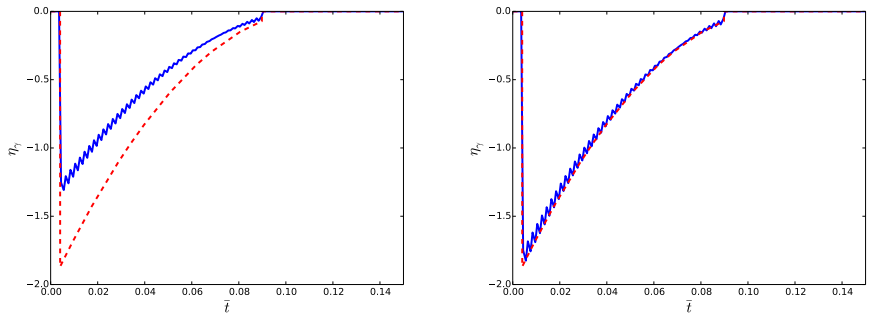

Figure 6. Evolution of the multiplier η_γ associated to the constraint c_γ. The solid blue lines represent the data extracted from direct method. Data in the rough ($\tilde{\eta}_i$) are presented on the left figure whereas processed data ($\eta_i = \tilde{\eta}_i h$, with h the step size) are presented on the right figure. The red dashed lines represent the multiplier from the discretization of the BVP problem (obtained with indirect method).

4.1.2. Hamiltonian associated to the constrained arc

The *HamPath* package computes the adjoint system by automatic differentiation from the true Hamiltonian. We need the following result which shows that one can replace the control and the multipliers by their parameterized formulations, given in section 3.6.2, in the Hamiltonian and then compute the adjoint system by differentiation, instead of doing the converse as the maximum principle indicates.

Proposition 4.2. *Let $c(x) \leqslant 0$ be a scalar constraint of order 1. We define for $z := (x, p) \in T^*M$ the true Hamiltonian*

$$\bar{H}_{\mathcal{C}}(z) := \bar{H}(z, u_2(x), \eta(z)) = H_0(z) + u_{1,\max} H_1(z) + u_2(x) H_2(z) + u_2(x)^2 H_3(z) + \eta(z)\, c(x)$$

with u_2 and η given in section 3.6.2. Let $\tilde{z} := (\tilde{x}, \tilde{p})$ such that $\varphi_2(\tilde{z}) = 0$ and $c(\tilde{x}) = 0$. Assuming $\varphi_1 > 0$, then there is exactly one extremal passing through $\tilde{z}$, such that $c = 0$ and $\varphi_2 = 0$ along the extremal, and it is defined by the flow of $\bar{H}_{\mathcal{C}}$.

Proof
First we show that the space $\Sigma := \{(x, p) \in T^*M, c(x) = 0, \varphi_2(x, p) = 0\}$ is invariant with respect to the flow of $\bar{H}_c$. Let $z(\cdot) := (x(\cdot), p(\cdot))$ be the integral curve of $\bar{H}_c$ passing through $\tilde{z} := (\tilde{x}, \tilde{p}) \in \Sigma$ at time $t = 0$. Let define $\Gamma := (\Gamma_1, \Gamma_2) \circ z(\cdot)$ with $\Gamma_1 := c \circ \pi_x$ and $\Gamma_2 := H_2 + 2(u_2 \circ \pi_x) H_3$, with $\pi_x(x, p) = x$. For readibility, we note c (resp. u_2) instead of $c \circ \pi_x$ (resp. $u_2 \circ \pi_x$) in the following calculus. Since Γ is differentiable, we have

$$\begin{aligned}
\frac{\mathrm{d}\Gamma_1 \circ z}{\mathrm{d}t}(t) &= \{\bar{H}_{\mathcal{C}}, \Gamma_1\}(z(t)) \\
&= \big(\underbrace{c' f}_{=0,\ \text{definition of } u_2} + (H_2 + 2u_2 H_3) \underbrace{\{u_2,\, \Gamma_1\}}_{=0} + \Gamma_1 \{\eta, \Gamma_1\} \big)(z(t)) \\
\frac{\mathrm{d}\Gamma_2 \circ z}{\mathrm{d}t}(t) &= \{\bar{H}_{\mathcal{C}}, \Gamma_2\}(z(t))
\end{aligned}$$

DOI: 10.1002/oca

$$=\big(\underbrace{H_{02}+u_{1,max}(H_{12}+2u_2H_{13})+2u_2H_{03}+u_2^2H_{23}+2H_3u_2'f}_{=\eta c'(f_2+2u_2f_3),\text{ by definition of }\eta}$$
$$-\eta c'(f_2+2u_2f_3)+\Gamma_2(\{u_2,H_2\}+2u_2\{u_2,H_3\})+\Gamma_1\{\eta,\Gamma_2\}\big)(z(t))$$

Then $\dot\Gamma(t)=A(t)\Gamma(t)$, with $A(t)=\begin{pmatrix}\{\eta,\Gamma_1\} & 0\\ \{\eta,\Gamma_2\} & \{u_2,H_2\}+2u_2\{u_2,H_3\}\end{pmatrix}(z(t))$. Since $\Gamma(0)=0$, $\Gamma\equiv 0$ and then $z(\cdot)$ remains in Σ. Besides,

$$\bar H_{\mathcal C}'(z)=\frac{\partial\bar H}{\partial z}(z,u_2(x),\eta(z))+\frac{\partial\bar H}{\partial u_2}(z,u_2(x),\eta(z))\,u_2'(x)+\frac{\partial\bar H}{\partial\eta}(z,u_2(x),\eta(z))\,\eta'(z)$$

with

$$\frac{\partial\bar H}{\partial u_2}(z,u_2(x),\eta(z))=\Gamma_2(z),\quad \frac{\partial\bar H}{\partial\eta}(z,u_2(x),\eta(z))=\Gamma_1(z).$$

So $\vec{\bar H}_{\mathcal C}(z(t))=\vec{\bar H}(z(t))$ as Γ_1 and Γ_2 vanish along $z(\cdot)$ and $(z(\cdot),(u_{1,max},u_2\circ x(\cdot)),\eta\circ z(\cdot))$ is extremal. □

4.1.3. Multiple shooting method

We define

$$\begin{aligned}H_+(z)&\coloneqq H(z,(u_{1,\max},\bar u_2(z)),0),\\ H_-(z)&\coloneqq H(z,(u_{1,\min},\bar u_2(z)),0),\\ H_\gamma(z)&\coloneqq H(z,(u_{1,\max},u_{2,\gamma}(z)),\eta_\gamma(z)),\\ H_v(z)&\coloneqq H(z,(u_{1,\max},u_{2,v}(z)),\eta_v(z)).\end{aligned}$$

the different true Hamiltonians related to the unconstrained cases (H_+, H_-), see section 3.5, and to the constrained cases (H_γ, H_v), see section 3.6.2. We define also the mapping $\exp\colon (t,z_0)\mapsto \exp(t\vec H)(z_0)$ which gives the solution at the time t of the Cauchy problem $\dot z(s)=\vec H(z(s))$, $z(0)=z_0$. We note $\sigma_1\sigma_2$ an arc σ_1 followed by an arc σ_2, σ_i denoting the projection $\pi_x(\exp(t\vec H_\alpha)(z_0))$ with $H_\alpha\in\{H_+,H_-,H_\gamma,H_v\}$.

The unconstrained case. We consider that we have only one unconstrained arc of the form σ_+. On this single arc, we need multilple shooting technique to deal with numerical instability arising from the singular perturbation. We note (z_i,t_i) the discretized points and times for multiple shooting. The times t_i are fixed and defined by $t_{i+1}=t_i+\Delta t$, $i=0,\dots,N-1$ with $\Delta t=t_f/(N+1)$. Then the multiple shooting function

$$S_1(p_0,t_f,z_1,\cdots,z_N)$$

is given by the following equations.

$$\begin{aligned}x_{1,f}&=\pi_{x_1}(z(t_f,t_N,z_N)),\quad x_{2,f}=\pi_{x_2}(z(t_f,t_N,z_N)),\\ x_{3,f}&=\pi_{x_3}(z(t_f,t_N,z_N)),\quad x_{5,f}=\pi_{x_5}(z(t_f,t_N,z_N)),\\ (\alpha-1)p^0&=\pi_{p_4}(z(t_f,t_N,z_N)),\quad -\alpha p^0=H_+(z(t_f,t_N,z_N)),\\ 0&=z(t_1,t_0,z_0)-z_1,\quad 0=z(t_2,t_1,z_1)-z_2,\quad\dots,\quad 0=z(t_N,t_{N-1},z_{N-1})-z_N,\end{aligned}$$

where $z_0\coloneqq(x_0,p_0)$, $z\colon (t_1,t_0,z_0)\mapsto\exp((t_1-t_0)\vec H_+)(z_0)$. A zero of S_1 gives a BC-extremal which satisfies the necessary conditions of the maximum principle defined in section 3.

DOI: 10.1002/oca

The constrained case. We consider an extremal of the form $\sigma_+\sigma_\gamma\sigma_+$ and we note $t_1 < t_2$ the switching times. From proposition 4.2 we only need to check $c_\gamma = 0$ and $\varphi_2 = 0$ at the entry-time of the boundary arc, *i.e* $c_\gamma(x(t_1)) = 0$ and $H_2(z(t_1)) + 2u_{2,\gamma}(x(t_1))H_3(z(t_1)) = 0$. From lemma 3.7, the jumps at times t_1 and t_2 are zero, *i.e.* $\nu_{t_1} = \nu_{t_2} = 0$. Due to numerical instability, mutliple shooting is also used on $[t_2, t_f]$ with $(t_{s,i}, z_{s,i})$ the discretized points and times (with $t_{s,0} = t_2$) such that $t_{s,i+1} = t_{s,i} + \Delta t$ for $i = 0, \ldots, N-1$ with $\Delta t = (t_f - t_2)/(N+1)$. In this case, the multiple shooting function

$$S_2 \coloneqq (p_0, t_1, t_2, t_f, z_1, z_2, z_{s,1}, \ldots, z_{s,N})$$

is given by the following equations.

$$\begin{aligned}
0 &= c_\gamma(\pi_x(z_1)), \quad 0 = H_2(z_1) + 2u_{2,\gamma}(\pi_x(z_1))H_3(z_1),\\
x_{1,f} &= \pi_{x_1}(z(t_f, t_{s,N}, z_{s,N})), \quad x_{2,f} = \pi_{x_2}(z(t_f, t_{s,N}, z_{s,N})),\\
x_{3,f} &= \pi_{x_3}(z(t_f, t_{s,N}, z_{s,N})), \quad x_{5,f} = \pi_{x_5}(z(t_f, t_{s,N}, z_{s,N})),\\
(\alpha-1)p^0 &= \pi_{p_4}(z(t_f, t_{s,N}, z_{s,N})), \quad -\alpha p^0 = H_+(z(t_f, t_N, z_{s,N})),\\
0 &= z(t_1, t_0, z_0) - z_1, \quad 0 = \exp((t_2 - t_1)\vec{H}_\gamma)(z_1) - z_2, \quad 0 = z(t_{s,1}, t_2, z_2) - z_{s,1},\\
0 &= z(t_{s,2}, t_{s,1}, z_{s,1}) - z_{s,2}, \ \ldots, \quad 0 = z(t_{s,N}, t_{s,N-1}, z_{s,N-1}) - z_{s,N},
\end{aligned}$$

where $z_0 \coloneqq (x_0, p_0)$, $z\colon (t_1, t_0, z_0) \mapsto \exp((t_1 - t_0)\vec{H}_+)(z_0)$. A zero of S_2 gives a BC-extremal satisfying the necessary conditions from section 3 and of the form $\sigma_+\sigma_\gamma\sigma_+$.

4.2. Numerical results

4.2.1. The problem ($\mathcal{P}_1$)

The unconstrained case. The shooting function S_1 defined in section 4.1.3 is implemented with data from Table III, $N = 16$ arcs and an initial mass of $x_{0,4} = 72\ 000$ kg. The Newton method algorithm used to find a zero of S_1 is initialized by data coming from direct methods (*Bocop*) and presented in section 2.3. Numerical integration is performed using the variable step-size scheme *radau5*, see [18]. The absolute and relative tolerances, used to compute the step size, are set repectively to 10^{-14} and 10^{-8}. The resulting unconstrained trajectory reaches the final manifold in $t_f = 696$ s and the aircraft consumed 964 kg of fuel. The corresponding states, adjoints, controls and constraints are displayed with solid lines on Figures 7 and 8. Let focus on Figure 7, the behavior of the altitude h and of the speed v are opposed at the beginning and at the end of the trajectory. At the beginning, the aicraft trades potential energy for kinetic energy in order to reach a sufficient climbing speed and at the end of the trajectory, the opposite exchange is realized in order to reach the targeted altitude. We can summarize this behaviour as an energy sharing strategy and even though this strategy fulfills the constraint c_v, it violates the constraint c_γ.

The constrained case. The result from direct method with the constraint on γ is given in the preliminary section 2.3, in Figure 3. From this figure, we deduce that the trajectory σ^* is composed by a concatenation of constrained and unconstrained arc such that $\sigma^* \coloneqq \sigma_+\sigma_\gamma\sigma_+$. The shooting function S_2 defined in section 4.1.3 is then implemented with data from Table III, $N = 17$ arcs and an initial mass of $x_{0,4} = 72\ 000$ kg. As for the unconstrained case, the Newton method used to find a zero of S_2 is initialized by data from *Bocop* and the numerical integration is performed by *radau5* code. The resulting trajectory reaches the targeted manifold in $t_f = 698$ s which is slighty superior than the unconstrained case but the aircraft still consumes around 964 kg of fuel. The red dashed lines on Figures 7 and 8 represent the constrained trajectory. The energy sharing strategy is used here at the end of the trajectory to gain potential energy and reach the targeted manifold.

4.2.2. The problem ($\mathcal{P}_{0.6}$)

DOI: 10.1002/oca

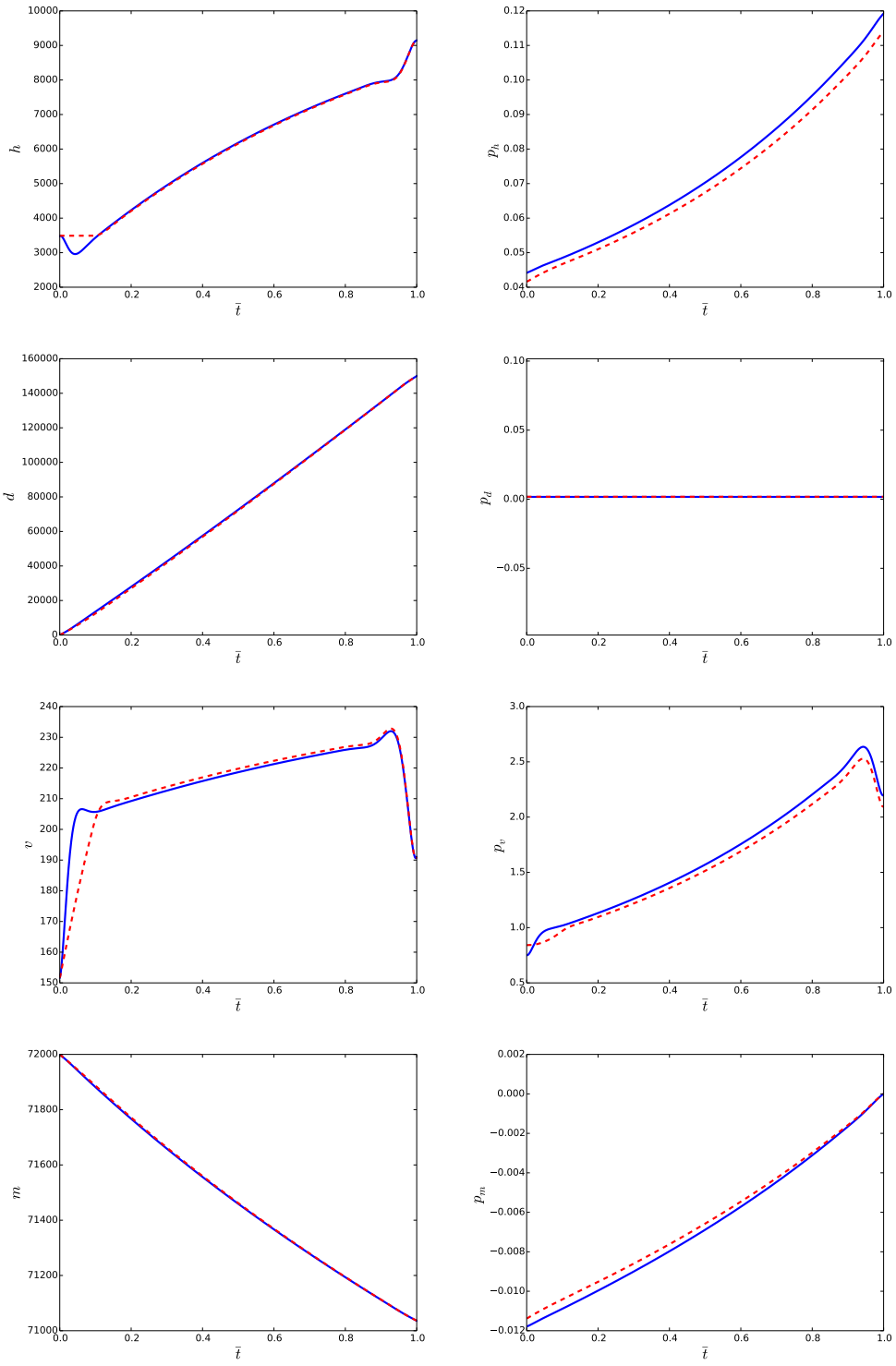

Figure 7. **Problem** ($\mathcal{P}_1$)**.** Evolution of the state (left) and adjoint (right) variables along the state unconstrained (blue plain lines) and the state constrained (red dashed lines) trajectories in the time minimal case with respect to the normalized time $\bar{t}$. From top to the bottom, we display the altitude h, the longitudinal distance d, the speed v and the mass m.

DOI: 10.1002/oca

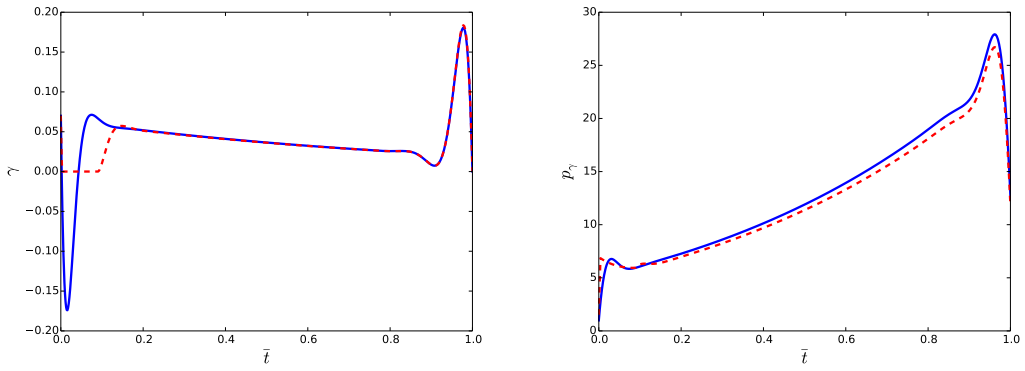

Figure 7. **Problem ($\mathcal{P}_1$).** Evolution of the air slope γ (left) and its associated adjoint p_γ (right) along the state unconstrained (blue solid lines) and the state constrained (red dashed line) trajectories with respect to the normalized time $\bar{t}$.

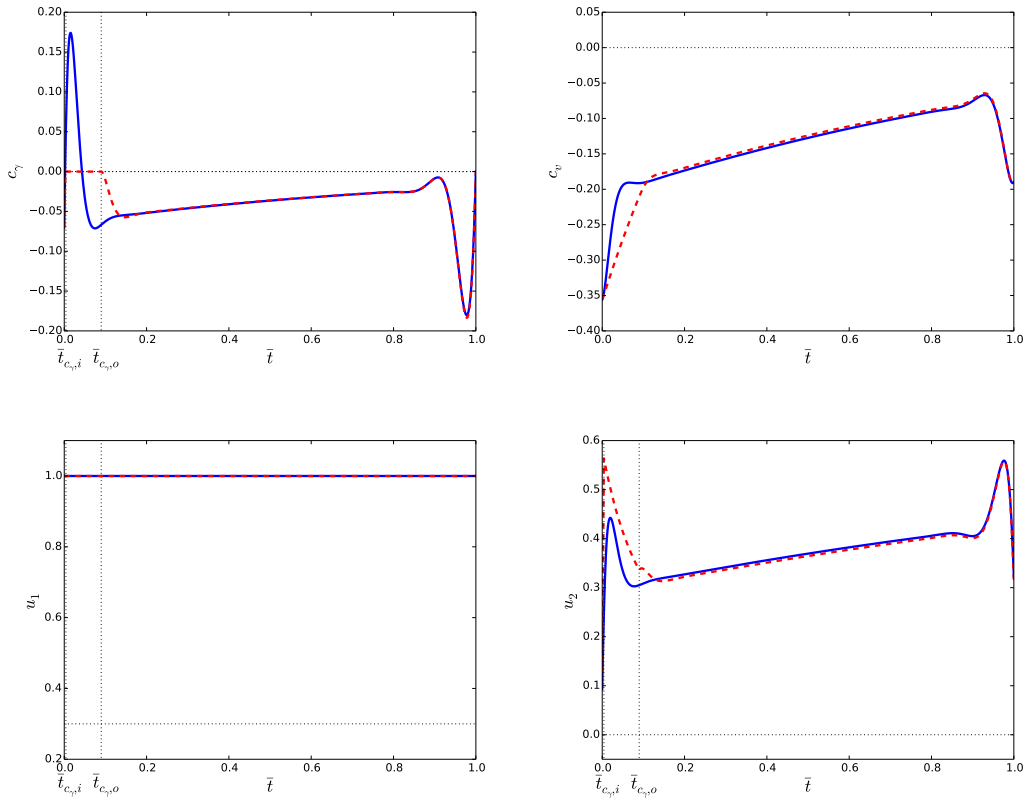

Figure 8. **Problem ($\mathcal{P}_1$).** Evolution of the constraints and the controls along the state unconstrained (blue solid lines) and state constrained (red dashed lined) trajectories with respect to the normalized time $\bar{t}$, in the time minimal case. From top left to bottom right, the constraint on the air slope (c_γ), the constraint on MACH speed (c_v), the thrust ratio (u_1) and the lift coefficient (u_2) are displayed. The time $\bar{t}_{c_{\gamma},i}$ (resp. $\bar{t}_{c_{\gamma},o}$) represents the entry (resp. the exit) time on the constraint c_γ. The horizontal black dotted lines represents the bounds of the constraints on the state and the control.

DOI: 10.1002/oca

The unconstrained case. The result from direct method for the problem $(\mathcal{P}_\alpha)$ with $\alpha = 0.6$ in the unconstrained case is given in Figure 4 (solid lines). From this figure, the trajectory is of the form $\sigma^* := \sigma_+\sigma_-$. In this case, the shooting function is clear. The difference from S_1 comes from the switching between σ_+ and σ_-. An additional condition is given by $H_1 = 0$ at the switching time t_1 which is an unknown of the shooting function in this case. This new function is then implemented using data from Table III, $N = 15$[¶] and with an initial mass of $x_{4,0} = 59\ 000$ kg. The data from *Bocop* and the code *radau5* are still used as an initial guess for the shooting method and to perform the numerical integration. The trajectory represented on Figures 9 and 10 by the blue solid lines is quite similar to the unconstrained case of the problem $(\mathcal{P}_1)$. It reaches the targeted manifold in $t_f = 650$ s with a fuel consumption of 873 kg. The observation of the Figure 10 shows that both constraints c_γ and c_v are violated by this trajectory but never simultaneously.

The constrained case. We deduce from the figure 4 and the unconstrained case that the trajectory is a concatenation of constrained and unconstrained arc such that $\sigma^* := \sigma_+\sigma_\gamma\sigma_+\sigma_v\sigma_-$. The corresponding shooting function is then adapted from the shooting function S_2 and is implemented using data from Table III and an initial mass of $x_{4,0} = 59\ 000$ kg. We split the second arc σ_+ and the arc σ_v in $N_+ = 12$ and $N_v = 10$ subarcs in order to deal with numerical instabilities. Like the other cases, data from *Bocop* are used as an initial guess to find a zero of the shooting function. The red dashed lines of Figures 9 and 10 depict the resulting trajectory. The final time $t_f = 654$ s is slightly superior than the final time in the unconstrained case, whereas the fuel consumption of 869 kg is slighty inferior. As for the problem $(\mathcal{P}_1)$, the constrained trajectory from $(\mathcal{P}_{0.6})$ follows the unconstrained one and the boundaries arcs do not modify the global behavior of the trajectory.

5. CONCLUSION

In this paper, the control problem of an aircraft in a climbing phase was modeled as a Mayer optimal control problem with two state constraints of order 1 and with affine and quadratic dependance with respect to the control. We have presented an approach which combines geometric analysis and numerical methods to compute candidates as minimizers which are selected among a set of extremals, solutions of a Hamiltonian system given by the maximum principle (section 3). The optimal trajectory is a concatenation of boundary and interior arcs. In section 3.6, we compute for each type of arcs we encounter in the numerical experiments, the control law, the multiplier associated to the constraint (scalar of order 1) and the jumps on the adjoint vector at junction times. Then we combined the theoretical results with indirect and direct methods to compute solutions which satisfy necessary conditions of optimality given by the maximum principle. One can find two technical results in section 4.1. First, proposition 4.1 justifies the use of the direct method to initialize the indirect method in the case of state constrained optimal control problems. It justifies also the direct adjoining approach, see 3.1. The second result from proposition 4.2 is a key tool for the definition of the multiple shooting functions which are solved by the indirect method, see section 4.1.3. At the end, we illustrate the approach with two examples: in section 4.2.1, we give a result about the minimum time problem while in section 4.2.2, one can find a more complex trajectory of the form $\sigma_+\sigma_\gamma\sigma_+\sigma_v\sigma_-$ in the case of a mixed criterion between time of flight and fuel consumption.

REFERENCES

1. P. R. Amestoy, I. S. Duff, J. Koster, and J.-Y. L'Excellent. A fully asynchronous multifrontal solver using distributed dynamic scheduling. *SIAM J. Matrix Anal. Appl.*, 23(1):15–41, 2001.
2. M. D. Ardema. Solution of the minimum time-to-climb problem by matched asymptotic expansions. *AIAA Journal*, 14(7):843–850, 1976.

[¶]The multiple shooting technique is only used along σ_+ since the arc σ_- is short.

DOI: 10.1002/oca

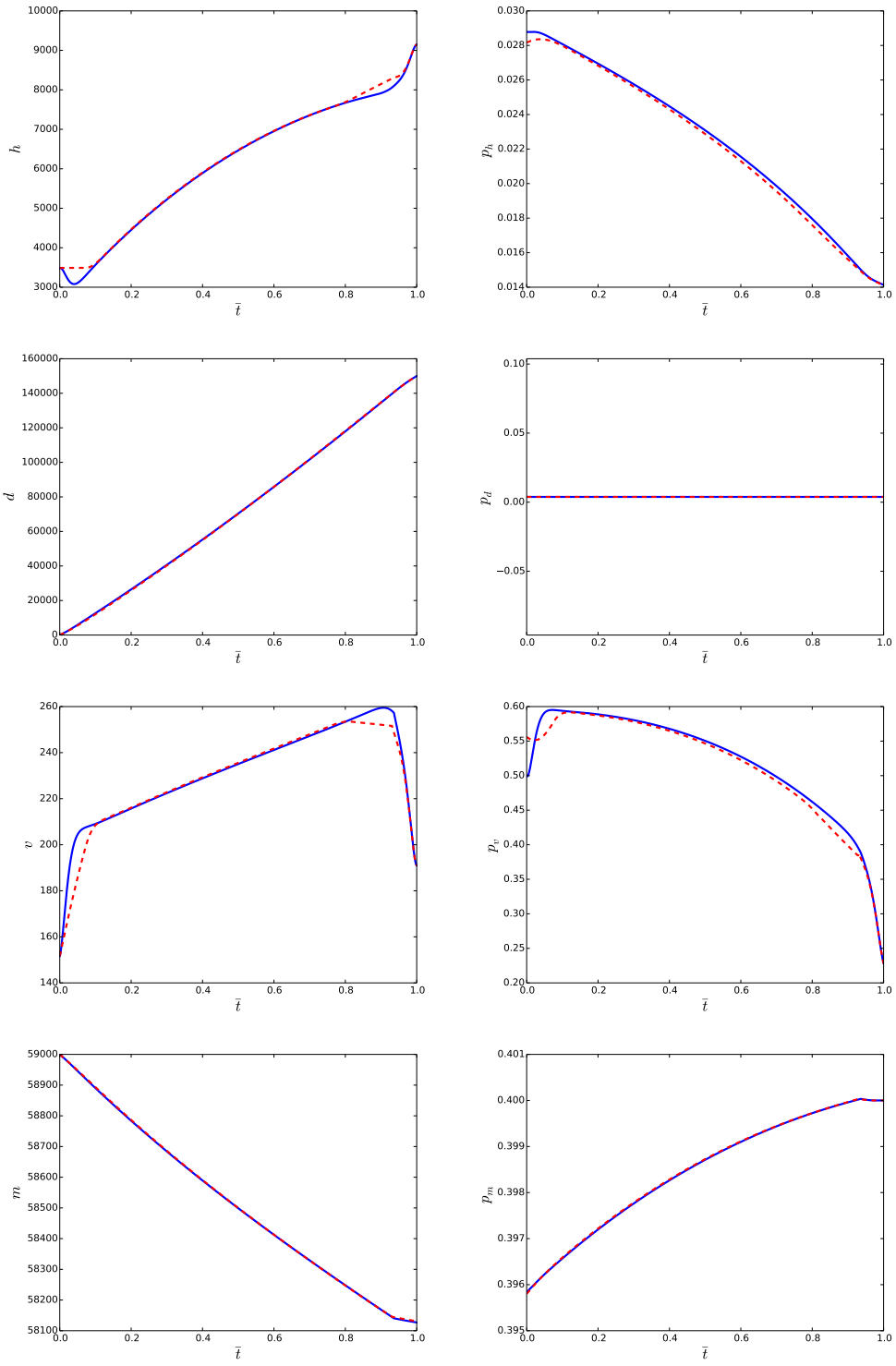

Figure 9. **Problem ($\mathcal{P}_{0.6}$).** Evolution of the state (left) and adjoint (right) variables along the state unconstrained (blue plain lines) and the state constrained (red dashed lines) trajectories in the mixed criterion problem ($\alpha = 0.6$) with respect to the normalized time $\bar{t}$. From top to the bottom, we display the altitude h, the longitudianl distance d, the speed v and the mass m.

DOI: 10.1002/oca

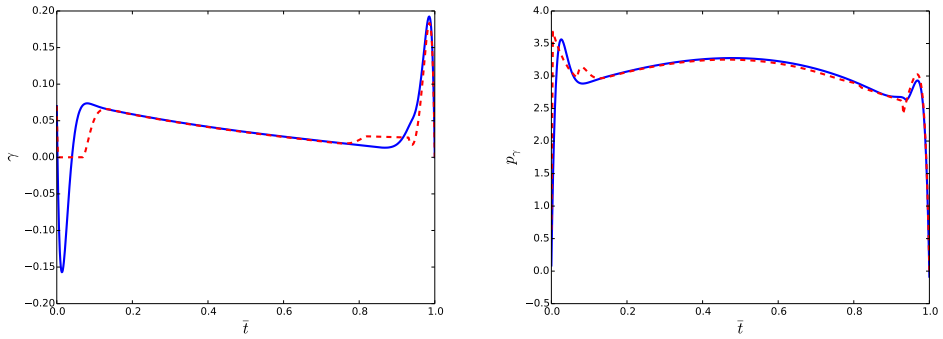

Figure 9. **Problem** ($\mathcal{P}_{0.6}$)**.** Evolution of the air slope γ (left) and its associated adjoint p_γ (right) along the state unconstrained (blue solid lines) and the state constrained (red dashed line) trajectories with respect to the normalized time $\bar{t}$.

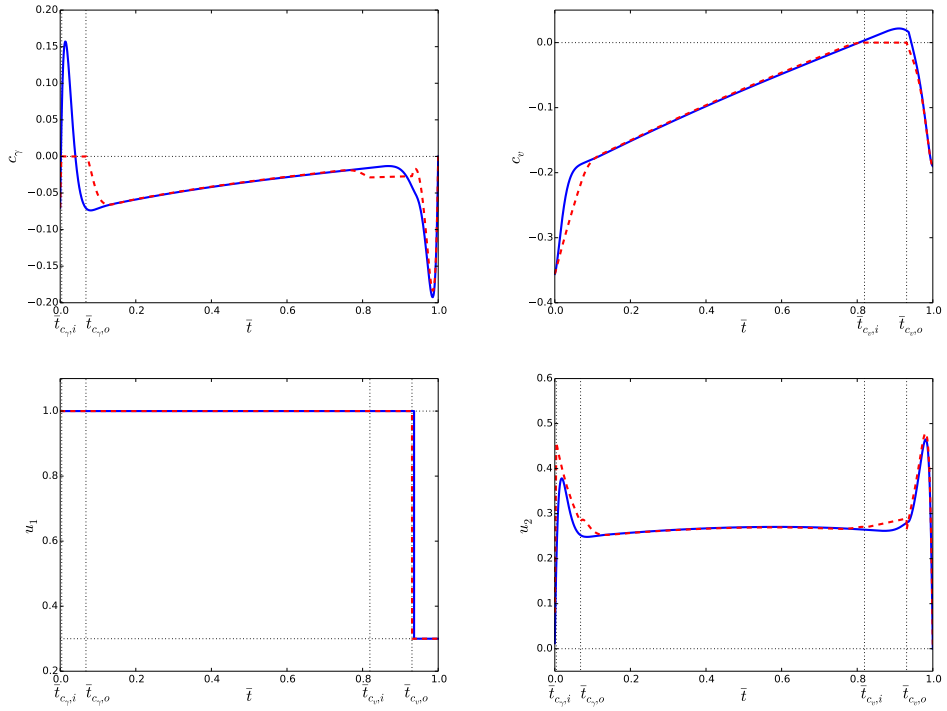

Figure 10. **Problem** ($\mathcal{P}_{0.6}$)**.** Evolution of the constraints and the controls along the state unconstrained (blue solid lines) and state constrained (red dashed lined) trajectories with respect to the normalized time $\bar{t}$ in the mixed criterion problem ($\alpha = 0.6$). From top left to bottom right, the constraint on the air slope (c_γ), the constraint on MACH speed (c_v), the thrust ratio (u_1) and the lift coefficient (u_2) are displayed. The time $\bar{t}_{c_{x,i}}$ (resp. $\bar{t}_{c_{x,o}}$), $x \in \{\gamma, v\}$, represents the entry (resp. the exit) time on the constraint c_x. The horizontal black dotted lines represents the bounds of the constraints on the state and the control.

3. J.T. Betts. *Practical Methods for Optimal control Using Nonlinear Programming*. Advances in Design and Control. Soc. for Industrial and Applied Math., Berlin, Heidelberg, New-York, 2001.
4. F. J. Bonnans, D. Giorgi, V. Grelard, S. Maindrault, and P. Martinon. Bocop - a collection of examples. Technical report, INRIA, july 2014.
5. J. F. Bonnans and A. Hermant. Well-posedness of the shooting algorithm for state constrained optimal control problems with a single constraint and control. *SIAM J. Control Optim.*, 46(4):1398–1430, 2007.
6. J. F. Bonnans and J. Laurent-Varin. Computation of order conditions for symplectic partitioned Runge-Kutta schemes with application to optimal control. Research Report RR-5398, INRIA, 2004.

DOI: 10.1002/oca

7. R. Bulirsch and J. Stoer. *Introduction to numerical analysis*, volume 12 of *Texts in Applied Mathematics*. Springer-Verlag New-York, third edition, 2002.
8. J.-B. Caillau, O. Cots, and J. Gergaud. Differential continuation for regular optimal control problems. *Optim. Methods Softw.*, 27(2):177–196, 2012.
9. J.R. Cash. The numerical solution of nonlinear two-point boundary value problems using iterated deferred correction - a survey. *Opuscula Math.*, 26(2), 2006.
10. O. Cots, J. Gergaud, and D. Goubinat. Time-optimal aircraft trajectories in climbing phase and singular perturbations (regular paper). In *IFAC World Congress, Toulouse, 09/07/2017-14/07/2017*, 2017.
11. A. L. Dontchev, W. Hager, and V. M. Veliov. Second-order Runge-Kutta approximations in constrained optimal control. *SIAM J. Numer. Anal.*, 38(1):202–226, 2000.
12. A. L. Dontchev and W. W. Hager. The Euler approximation in state constrained optimal control. *Math. Comp.*, 70(233):173–203, 2001.
13. F. Fahroo and I.M. Ross. Legendre Pseudospectral Approximations of Optimal Control Problems. *Lecture Notes in Control and Inform. Sci.*, 295, 2003.
14. M. Gerdts. *Optimal control of ODEs and DAEs*. De Gruyter Textbook, 2011.
15. D. Goubinat. *Contrôle optimal géométrique et méthodes numériques : application au problème de montée d'un avion*. PhD thesis, INP-ENSEEIHT-IRIT, 2017.
16. W. Hager. Runge-Kutta methods in optimal control and the transformed adjoint system. *Numer. Math.*, 87(2):247–282, 2000.
17. E. Hairer, C. Lubich, and G. Wanner. *Geometric Numerical Integration. Structure–Preserving Algorithms for Ordinary Differential Equations*, volume 31 of *Springer Series in Computational Mathematics*. Springer-Verlag Berlin Heidelberg, second edition, 2006.
18. E. Hairer and G. Wanner. *Solving ordinary differential equations II. Stiff and differential-Algebraic Problems*. Springer series in computational mathematics. Springer, Heidelberg, 2010.
19. R.F. Hartl, S.S. Sethi, and R.G. Vickson. A survey of the maximum principles for optimal control problems with state constraints. *SIAM Review*, 37(2):181–218, 1995.
20. L. Hascoët and V. Pascual. The Tapenade Automatic Differentiation tool: Principles, Model, and Specification. *ACM Trans. Math. Software*, 39(3), 2013.
21. J.K. Hunter. Asymptotic analysis and singular perturbation theory. Technical report, University of Californi at Davis, Department of Mathematics, February 2004.
22. A. D. Ioffe and V. M. Tikhomirov. *Theory of extremal problems*. Studies in mathematics and its applications. North-Holland Pub. Co. New York, Amsterdam, New York, 1979.
23. D.H. Jacobson, M.M. Lele, and J.L. Speyer. New necessary conditions of optimality for control problems with state-variable inequality constraints. *J. Math. Anal. Appl.*, 35:255–284, 1971.
24. J. Laurent-Varin. *Calcul de trajectoires optimales de lanceurs spatiaux réutilisables par une méthode de point intérieur*. Thèse de doctorat, École Polytechnique, novembre 2005.
25. H. Maurer. On optimal control problems with bounded state variables and control appearing linearly. *SIAM J. Cont. Optim.*, 15(3):345–362, 1977.
26. N. Moissev. *Problèmes mathématiques d'analyse des systèmes*. Mir Moscou, 1985.
27. J. J. Moré, B. S. Garbow, and K. E. Hillstrom. User guide for minpack-1. Technical Report ANL-80-74, Argonne National Library, 1980.
28. N. Nguyen. Singular arc time-optimal climb trajectory of aircraft in a two-dimensional wind field. In *AIAA Guidance, Navigation and Control Conference and Exhibit*, Guidance, Navigation, and Control and Co-located Conferences, august 2006.
29. R.E. O'Malley. *Singular Perturbation Methods for Ordinary Differential Equations*. Springer-Verlag New-York, 1991.
30. D. Poles. Base of aircraft data (BADA) aircraft performance modelling report. EEC Technical/Scientific Report 2009-09, Eurocontrol, september 2009.
31. L. Pontriaguine, V. Boltianski, R.Gamkrélidizé, and E. Mitchenko. *Théorie mathématiques des processus optimaux*. Editions Mir, Moscou, 1974.
32. A.V. Rao. A survey of numerical methods for optimal control. *2009, AAS/AIAA Astrodynamics Specialist Conference*, AAS Paper 09-334, Pittsburgh, PA, August 10 - 13, 2009.
33. I.M. Ross. *A Primer on Pontryagin's Principle in Optimal Control*. Collegiate Publisher, 2015.
34. A. Wachter and L. T. Biegler. On the implementation of a primal-dual interior point filter line search algorithm for large-scale nonlinear programming. *Math. Program.*, 106(1):25–57, 2006.
35. A. Walther and A. Griewank. Getting started with adol-c. *Combinatorial Scientific Computing, Chapman-Hall CRC Computational Science*, pages 181–202, 2012.

DOI: 10.1002/oca